Journal of Dental Sciences 20 (2025) 539–552

Available online at www.sciencedirect.com

ScienceDirect

journal homepage: www.e-jds.com

Original Article

Beta-adrenergic receptor antagonist propranolol prevents bisphosphonate-related osteonecrosis of the jaw by promoting osteogenesis

Qianxin Du [a,b†], Qizhang Wang [a,b†], Yuhao Wang [a,b], Chengzhi Zhao [a,b], Jian Pan [a,b*]

[a] State Key Laboratory of Oral Diseases & National Clinical Research Center for Oral Diseases, West China Hospital of Stomatology, Sichuan University, Chengdu, China
[b] Department of Oral and Maxillofacial Surgery, West China Hospital of Stomatology, Sichuan University, Chengdu, China

Received 1 April 2024; Final revision received 18 April 2024
Available online 4 May 2024

KEYWORDS
Bisphosphonate-related osteonecrosis of the jaw (BRONJ);
Zoledronic acid;
Tooth extraction;
Propranolol;
Beta-adrenergic receptor

Abstract *Background/purpose:* Bisphosphonate-related osteonecrosis of the jaw (BRONJ), a complication arising from the use of bisphosphonates (BPs), inflicts long-term suffering on patients. Currently, there is still a lack of effective treatments. This study aimed to explore the preventive effects of propranolol (PRO) on BRONJ in vitro and in vivo, given PRO's potential in bone health enhancement.

Materials and methods: In vitro, effect of PRO on zoledronic acid (ZA)-pretreated bone marrow mesenchymal stem cells (BMSCs) was detected by cell counting kit-8, alkaline phosphatase (ALP) staining, alizarin red staining, real-time quantitative polymerase chain reaction (RT-qPCR) and Western blot. In vivo, forty mice were divided into four groups: control, ZA, PRO, and ZA-PRO. The maxillary extraction sockets sides were analyzed with micro-CT and histomorphometry. Hematoxylin-eosin (H&E), Masson staining, immunofluorescence staining of ALP, bone morphogenetic protein 2 (BMP2), runt-related transcription factor 2 (RUNX2) and TUNEL staining were performed.

Results: PRO increased proliferation and osteogenic differentiation of BMSCs. PRO stimulated bone formation and facilitated the healing process in zoledronic acid-induced osteonecrosis of jaw in mouse model. Compared with ZA group, control and PRO group showed more $BMP2^{+}$, $RUNX2^{+}$, and ALP^{+} cells ($P < 0.05$). However, PRO rescued the decreased expression of ALP, RUNX2, BMP2 due to ZA and decreased the expression of TUNEL ($P < 0.05$).

* Corresponding author. West China Hospital of Stomatology, Sichuan University, No.14, Section 3rd, Renmin Nan Road, Chengdu, 610041, China.
E-mail address: jianpancn@scu.edu.cn (J. Pan).
† These authors contributed equally to this work.

https://doi.org/10.1016/j.jds.2024.04.016

Conclusion: The findings suggest that propranolol may offer a promising preventive strategy against BRONJ by enhancing bone regeneration. This research contributes to the understanding of the pathogenesis of BRONJ and opens avenues for potential treatments of BRONJ focusing on β-adrenergic signaling.

Introduction

Bisphosphonates (BPs) are widely used in clinical practice for the prevention and treatment of diseases such as osteoporosis and malignant tumor bone metastasis due to their excellent anti-bone resorption effect.[1] However, long-term use of BPs may lead to complications of jawbone necrosis, clinically manifested as facial pain, exposure of dead bones, and persistent fistulas. In 2007, the American Association of Oral and Maxillofacial Surgeons (AAOMS) officially defined this condition as bisphosphonate-related osteonecrosis of the jaws (BRONJ).[2] Subsequently, other anti-resorptive agents such as denosumab, as well as targeted anti-angiogenic drugs in tumor treatment, were also found to cause osteonecrosis of jaws. Therefore, in 2014, AAOMS renamed BRONJ as medication-related osteonecrosis of the jaws (MRONJ).[3] With the popularization of the use of related drugs, such patients have increased significantly in clinical practice. Among them, the incidence rate of MRONJ is 0.3%—5% for patients receiving intravenous zoledronic acid (ZA) (one of the most frequently used BPs).[4—6] After more than two years of intravenous ZA treatment the incidence rate of MRONJ has increased to 3.8%—18%.[7] In addition to surgery, non-surgical treatments mainly include the use of antibiotics, hyperbaric oxygen therapy, combination of pentoxifylline and tocopherol, teriparatide, etc.[8] However, there is currently no significant treatment method available. The prevention and treatment methods for this disease are still under continuous research.

The pathogensis of MRONJ remains elusive, but several theories have been proposed to explain its development. These include: the suppression of bone turnover, hindrance of new blood vessel formation, bacterial infections in the oral cavity, reduced immune system efficacy, toxic effects on cells, the occurrence of tiny fractures in the jawbone, and variations in individual genes known as single nucleotide polymorphisms (SNPs).[9] The theory of bone remodeling inhibition suggests that bone remodeling of jaw is based on the functional coupling between osteoblasts and osteoclasts. Both BPs and denosumab inhibit the function of osteoclasts, leading to impaired osteoblast function and disrupted bone metabolism, ultimately inducing MRONJ. The mechanism of inducing MRONJ by regulating osteoclasts has been extensively studied,[10] but there is no mature prevention and treatment method based on this mechanism for clinical use. Therefore, research on the pathogenesis of MRONJ should not be limited to osteoclasts alone. The impact of related drugs on bone metabolism balance is a possible future research direction.[11—14]

As a target organ of the nervous system, bones are innervated by the sympathetic nervous system (SNS). Numerous studies have clarified the important role of SNS in bone metabolism.[15—17] Interfering with the sympathetic nerve signals has emerged as a potential strategy to enhance bone health, given that overstimulation of the sympathetic nerves and the resultant overproduction of catecholamines by these nerves can negatively impact bone integrity.[18,19] Within this system, adrenergic receptors, categorized as G protein-coupled receptors, are divided into α and β. The β-adrenergic receptors (β-ARs) found on osteoblasts and osteoclasts play a crucial role in the sympathetic regulation of bone metabolism.[20] Activation of β-ARs on osteoblast surfaces leads to the inhibition of the phosphorylation of the cAMP response element-binding protein, which in turn suppresses cellular differentiation and reduces bone formation.[21] When β-ARs on the surface of osteoclasts are activated, this promotes osteoclast differentiation, reducing bone mass and density.[22] Furthermore, the activation of β-ARs also exerts an inhibitory effect on the osteogenic differentiation of bone marrow mesenchymal stem cells (BMSCs) via the cAMP/PKA signaling pathway.[23] Propranolol (PRO), a widely used non-selective β adrenergic receptor blocker in clinical practice, can block both β1-AR and β2-AR. Researchers have found that elderly cardiovascular disease patients taking propranolol have significantly reduced risks of osteoporosis and fractures,[24] suggesting that while treating cardiovascular diseases, it also helps prevent diseases such as osteoporosis. And it has been shown to enhance bone healing and implant osseointegration in rats.[25] These properties indicate that PRO may restore extraction socket healing in BRONJ lesions by promoting osteogenesis.

This study aimed to investigate the preventive effects of PRO on ZA-pretreated BMSCs and on osteonecrosis of the jaw induced by ZA in a mouse model. The research was grounded in the hypothesis that PRO promotes osteogenic differentiation of BMSCs, augments bone formation, and supports the healing of extraction sockets in live models affected by BRONJ.

Materials and methods

Cell culture, treatments and osteoinduction

Male Sprague—Dawley rats, aged three weeks, were euthanized via cervical dislocation, and the tibiae were isolated to harvest BMSCs. The BMSCs were cultured in high-glucose Dulbecco's Modified Eagle Medium (Gibco BRL,

Gaithersburg, MD, USA) supplemented with 15% fetal bovine serum (Cell-box, Changsha, China) and 1% penicillin/streptomycin (Gibco BRL). BMSCs were incubated at 37 °C in a humidified atmosphere containing 5% CO2, with the medium being replaced every 48 h. Cells were passaged at a ratio of 1:3. Passage 3 (P3) BMSCs were used for subsequent experiments.

P3 BMSCs were osteoinduced by osteogenic induction medium (OIM) which contained 50 μg/ml ascorbic acid (Solarbio, Beijing, China), 10 mM β-glycerol phosphate (Sigma–Aldrich, St. Louis, MO, USA), and 10 nM dexamethasone (Solarbio). P3 BMSCs divided into six groups, each group was undergone osteogenic induction and treated with 50 nM isoproterenol (ISO, GLPBIO, Montclair, CA, USA) to simulate sympathetic nervous system activity in the body: (i) control; (ii) BMSCs incubated with 1 μM PRO (GLPBIO); (iii) BMSCs incubated with 10 μM PRO; (iv) BMSCs preincubated with 10 μM ZA (MedChemExpress, Monmouth Junction, NJ, USA) for 24 h; (v) BMSCs preincubated with 10 μM ZA for 24 h and then treated with 1 μM PRO; (vi) BMSCs preincubated with 10 μM ZA for 24 h and then treated with 10 μM PRO. During osteogenic induction, medium was changed every 48 h.

Cytotoxicity assays

Cytotoxicity tests of ZA, PRO, and ISO were determined using the Cell Counting Kit-8 assay (CCK-8, APExBIO, Houston, NJ, USA). P3 BMSCs were plated at a density of 3.5 × 103 cells per well in 96-well plates. At various time points (24, 48, and 72 h) following treatment with different concentrations of ZA, PRO, and ISO, the medium was removed and the cells were gently washed with phosphate buffer saline (PBS, Biosharp, Hefei, China). Following this, each well received 100 μl of 10% CCK-8 medium, and the plates were then incubated at 37 °C for 1 h. The absorbance at 450 nm was subsequently measured with a microplate reader (SpectraMax iD3, Molecular Devices, San Jose, CA, USA).

Alkaline phosphatase (ALP) staining

P3 BMSCs were plated at a density of 1.5 × 105 cells per well in six-well plates. After osteogenic induction of 14 days, the cells were fixed with 4% paraformaldehyde and subsequently washed three times. Staining was performed for approximately 30 min using the BCIP/NBT Alkaline Phosphatase Color Development Kit (C3206, Beyotime, Shanghai, China) until the color development met the desired criteria. The reaction was halted, the working solution was discarded, and the wells were washed thrice before observations and photographic documentation were carried out under a microscope.

Alizarin red S staining

P3 BMSCs were seeded at a concentration of 1.5 × 105 cells per well into six-well plates. After osteogenic induction of 14 days, the cells were fixed using 4% paraformaldehyde, followed by three washes. Staining was conducted for 5 min using Alizarin Red S Solution (G1452, Solarbio), after which the dye was discarded, and the cells were washed five times. Observations and imaging were then performed under a microscope.

Real-time quantitative polymerase chain reaction (RT-qPCR)

After 7 or 14 days of induction under varying conditions, total RNA from BMSCs was isolated using the Cell Total RNA Isolation Kit (Foregene, Chengdu, China). This was followed by the synthesis of complementary DNA (cDNA) via reverse transcription using the RT Easy II kit (Foregene). Quantification of the cDNA was performed through RT-qPCR experiments utilizing the Real Time PCR Easy-SYBR Green I Kit (Foregene). At day 7, the gene expressions of runt related transcription factor 2 (*Runx2*) and bone morphogenetic protein 2 (*Bmp2*) were evaluated as indicators of early osteogenesis, while the expression of osteopontin (*Opn*) at day 14 served as a marker for late-stage osteogenesis. Glyceraldehyde-3-phosphate dehydrogenase (*Gapdh*) was employed as the housekeeping gene for normalization purposes. All experiments were replicated three times. The sequences of the primers used are provided in Table 1.

Western blot

After 7 or 14 days of induction in various conditions, total protein was extracted from the BMSCs using the Total Protein Extraction Reagent (Signalway Antibody, Greenbelt, MD, USA). Protein samples were prepared for denaturation by adding a 1:4 volume of 5X loading buffer (EpiZyme, Shanghai, China) and subjecting them to a 99 °C metal bath for 10 min. Equal amounts of denatured protein were then loaded onto a 10% polyacrylamide gel electrophoresis gels (EpiZyme) for electrophoresis, followed by transfer to a PVDF membrane (Merck Millipore, Burlington, MA, USA). The membranes were probed with anti-RUNX2 (ET1612-47, 1:1000, Huabio, Hangzhou, China), anti-BMP2 (ER80602, 1:1000, Huabio), anti-OPN (0806-6, 1:1000, Huabio), and anti-GAPDH (ET1601-4, 1:1000, Huabio), as well as goat anti-rabbit secondary antibodies (HA1006, 1:10000, Huabio). The membranes were then incubated with chemiluminescence (ECL) reagent (Abbkine, Atlanta, GA, USA) and the images were captured using the ChemiDoc Touch

Table 1 Primers used for RT-qPCR.

Genes	Primers (5′– 3′) (F: forward; R: reverse)
Bmp2	F:ACACAGGGACACACCAACCAT
	R:TGTGACCAGCTGTGTTCATCTTG
Gapdh	F:AGTGCCAGCCTCGTCTCATA
	R:GGGTTTCCCGTTGATGACCA
Opn	F:CAGTCGATGTCCCTGACGG
	R:GTTGCTGTCCTGATCAGAGG
Runx2	F:CACAAGTGCGGTGCAAACTT
	R:AATGACTCGGTTGGTCTCGG

Bmp2: bone morphogenetic protein 2. *Gapdh*: glyceraldehyde-3-phosphate dehydrogenase. *Opn*: osteopontin. *Runx2*: runt related transcription factor 2.

chemiluminescent imaging system (Bio-Rad, Hercules, CA, USA).

Bisphosphonate-related osteonecrosis of the jaw model establishment and treatment with propranolol

The Ethics Committee granted approval for this experiment under the protocol number 20220402001, which was conducted at the Experimental Animal Center of West China Hospital, Sichuan University. In this study, forty 8-week-old male C57BL/6 mice, with weights ranging between 18 and 22 g, were randomly divided into four experimental groups: (i) control, (ii) ZA, (iii) PRO, and (iv) ZA-PRO. To increase the prevalence of osteonecrosis, the corticosteroid drug dexamethasone was utilized.[26] Dexamethasone (DX, Solarbio) was administered intraperitoneally (i.p.) at a dose of 2 mg/kg to each mouse twice weekly for a duration of four weeks. Additionally, the ZA and ZA-PRO groups were treated with ZA (200 μg/kg, i.p., twice a week), while the PRO and ZA-PRO groups received PRO (20 mg/kg, i.p., twice a week) under the same schedule for four weeks prior to tooth extraction. The tooth extractions were conducted in the fifth week, after the four-week administration of DX, ZA, and PRO. The procedure involved separating the gingiva surrounding the molars with a dental explorer and extracting the right maxillary first and second molars using Adson forceps (straight head with a 0.6 mm hook). To halt bleeding, cotton balls were applied to the extraction sites. Following tooth extraction, the PRO and ZA-PRO groups continued to receive PRO (20 mg/kg, i.p.) twice weekly for an additional two weeks. At the same time, mice in both the control group and the ZA group received an identical volume of saline i.p. After this period, the mice were euthanized, and their maxillae were collected for further detection and analysis.

Micro-CT analysis

Specimen analysis was performed using a Micro-CT scanner (Scanco Medical AG, Zurich, Switzerland) with 55 kVp/145 μA, 10 μm voxel size. Measurements and analyses of bone volume to tissue volume (BV/TV), number of trabecular (Tb. N), thickness of trabeculae (Tb. Th), and separation of trabeculae (Tb. Sp) were carried out on the reconstructed volumes of interest.

Hematoxylin-eosin (H&E) and Masson staining

Every maxilla was thoroughly fixed in paraformaldehyde, subsequently decalcified using 10% ethylene diamine tetraacetic acid, dehydrated through an alcohol series, cleared in xylene, and finally embedded in paraffin. For histological examination, serial sagittal slices 5-μm thick were prepared, cutting through the mesial—distal axis of the right maxillary molars.

Following the removal of wax using xylene, specimens were subjected to an alcohol gradient for rehydration, then washed and stained with hematoxylin for 20 min. After staining, they were rinsed under running water for 15 min and differentiated with 0.5% hydrochloric acid in ethanol for 30 s, followed by a 15-min immersion in tap water. Subsequently, the slides were stained with Eosin solution for 2 min. A conventional dehydration process using a gradient alcohol series was then performed, after which the slides were cleared in two xylene solutions for 5 min each. Finally, the slides were sealed with neutral balsam, and images were captured and analyzed.

Tissue sections underwent deparaffinization and hydration before staining with Weigert's Iron Hematoxylin for 5—10 min. Differentiation was carried out with acidic ethanol differentiation solution for 2—10 s, followed by a water rinse. Masson's Blueing Solution was applied, followed by a 1-min distilled water rinse. Sections were stained with Biebrich Scarlet-Acid Fuchsin for 5—10 min, then rinsed with a weak acid solution. After phosphomolybdic acid and weak acid washes, Aniline Blue staining was performed for 1—2 min. Sections were rapidly dehydrated with 95% ethanol and cleared with xylene before being mounted with neutral gum.

Immunofluorescence staining

Firstly, the slides were dewaxed using xylene and then rehydrated through a series of alcohol concentrations. After washing, drop 20 ug/ml Protease K (APExBIO) solution onto the tissue and incubate at 37 °C for 20 min for antigen retrieval. After natural cooling, the sections were washed three times with PBS for 5 min each. Tissue sections were then incubated in 5% bovine serum albumin (BSA, BioFroxx, Heidelberg, Germany) for 1 h at ambient temperature to block non-specific binding sites, followed by rinses with ddH2O and PBS (Biosharp). Overnight incubation with the primary antibody (1:200, Huabio) at 4 °C in a humidified chamber. After rinsing thrice with PBS (Biosharp) for 5 min each, sections were incubated with a fluorescent secondary antibody (1:500, A23240, Abbkine) in a wet box at room temperature for 1 h. Finally, the slides were sealed with antifade mounting medium containing DAPI (Abbkine) and stored at −4 °C and filmed with a spinning-disk confocal microscope (SpinSR10, Olympus, Tokyo, Japan).

Terminal deoxynucleotidyl transferase-mediated deoxyuridine triphosphate nick end-labeling (TUNEL) staining

TUNEL and immunofluorescence co staining were carried out according to protocol of the TUNEL staining kit (APExBIO). The steps in the previous section are as described earlier. After sealing with 5% BSA (BioFroxx) for 1 h, incubated with 1 × Equilibration Buffer at room temperature for 20 min and then removed it. Incubated with terminal deoxynucleotidyl transferase (TdT) working solution at 37 °C for 1 h in a dark wet box. Subsequently, as described earlier, the samples were washed with PBS and then incubated overnight with the primary antibody at 4 °C in a wet box.

Statistical analysis

In this study, at least three parallels were set for each experimental group, and all data were represented as mean ± standard deviation (SD). Quantitative analysis of relevant images was conducted using Image J software (National Institutes of Health, Bethesda, MD, USA).

Univariate analysis of variance and Tukey test analysis were performed on all data using GraphPad Prism 9.0.0 software (GraphPad Software, Inc., San Diego, CA, USA). The statistical significance tested were $^{*}P < 0.05$, $^{**}P < 0.01$ and $^{***}P < 0.001$ respectively.

Results

Effects of zoledronic acid, propranolol, and isoproterenol on cell viability

To explore the effects of ZA, PRO, and ISO on the viability of BMSCs, cells were treated with various concentrations of the drugs (ZA: 1 μM, 10 μM, 100 μM; PRO: 0.1 μM, 1 μM, 10 μM; ISO: 50 nM) and subjected to CCK-8 assays at different time points (24, 48, 72 h). The results indicated that the cytotoxicity of ZA on BMSCs became more pronounced with increasing concentrations of ZA and longer duration of treatment. 100 μM ZA and prolonged treatment durations significantly impaired cell proliferation ($P < 0.001$) (Fig. 1a). Consequently, we selected the experimental condition of pre-treatment with 10 μM ZA for 24 h for the remaining in vitro studies. Additionally, it was found that 1 μM PRO significantly enhanced the proliferation of BMSCs ($P < 0.05$), while 10 μM PRO and 50 nM ISO did not adversely affect the proliferation of BMSCs ($P > 0.05$) (Fig. 1b). Thus, these concentration conditions were used in subsequent experiments.

Propranolol restored bone marrow mesenchymal stem cells osteogenesis that was inhibited by zoledronic acid

The osteogenic capacity of BMSCs following interventions under different conditions was assessed through ALP staining, Alizarin Red staining, RT-qPCR, and western blots. The results from Alizarin Red staining and its quantitative analyses indicated that 1 μM PRO demonstrated a superior ability to promote osteogenic differentiation of BMSCs compared to 10 μM PRO ($P < 0.01$) (Fig. 1c–e). Simultaneously, ZA significantly reduced ALP activity ($P < 0.05$) and calcium nodule formation ($P < 0.001$); however, the addition of 1 μM PRO notably counteracted the suppressive impact of ZA on the osteogenic differentiation potential of BMSCs ($P < 0.01$, $P < 0.001$) (Fig. 1c–f). Similarly, when compared to the control and ZA group, both the 1 μM PRO group and the ZA + 1 μM PRO group showed significant upregulation in the expression levels of osteogenesis-related genes (*Runx2*, *Bmp2*, and *Opn*) and proteins (RUNX2, BMP2, and OPN) (Fig. 1g–i). These results suggest that 1 μM PRO possesses a potent osteogenic promoting effect on BMSCs and can recover the impairment of osteogenic capacity in BMSCs caused by ZA.

Distribution of tyrosine hydroxylase-positive nerve fibers and β2-adrenergic receptors in the maxillary molar region

Our initial investigation focused on the SNS innervation patterns within the mandibular molar area. We utilized sections from C57BL/C mice, which were then stained to identify the sympathetic marker tyrosine hydroxylase (TH). The TH-positive tissues in the images represent cross-sections of sympathetic neurons, appearing as punctate structures surrounding blood vessels (Fig. 2a). This indicates that sympathetic nerves innervate the tissues around the mandibular molars and are closely associated with the vascular system. The localization of β2-ARs on bone tissue cells in the molar region was demonstrated, showing their distribution along the bone trabeculae (Fig. 2b). To evaluate whether treatment measures in different groups affected the expression of β2-ARs on bone tissue cells, a quantitative analysis was further conducted. The results indicated that there was no significant difference in the proportion of $\beta2\text{-AR}^{+}$ cells among the groups ($P > 0.05$) (Fig. 2c and d). These anatomical structures are the foundation of this study.

Clinical-macroscopic evaluation and Micro-CT analysis of BRONJ lesions

The establishment of MRONJ animal model and drug injection process are shown in the following figure (Fig. 3a). The criteria for successful healing of the tooth extraction socket included the absence of a visible socket to the naked eye, full coverage by mucosa, lack of significant inflammation, and the invisibility of necrotic bone. The findings of this study indicated that the control group and the PRO group demonstrated superior soft tissue recovery at the extraction sites. Conversely, in the ZA group, there was a clear exposure of necrotic bone, with the extraction sites not being adequately covered by soft tissue. Meanwhile, the ZA-PRO group displayed a minor extent of bone exposure (Fig. 3b). The rates of bone exposure of ZA and ZA-PRO groups was 60% and 20% respectively (Fig. 3c).

Micro-CT was utilized to three-dimensionally reconstruct and quantitatively assess bone regeneration in extraction sockets. Both the control and PRO groups exhibited complete healing, with the sockets being entirely filled by regenerated bone. In contrast, the ZA group showed inadequate healing with minimal new bone formation. However, in the ZA-PRO group, new bone formation was noticeable, and the sockets were nearly completely healed (Fig. 3d). Furthermore, a statistical analysis of the micro-CT data was conducted. The bone volume fraction (BV/TV), representing the amount of trabecular bone in the samples, was calculated. The BV/TV values for the control, PRO, ZA, and ZA-PRO groups were 61%, 66.67%, 40.25%, and 52.83%, respectively, demonstrating that the quantitative findings align with the reconstruction observations. The BV/TV and Tb.Sp in the ZA group showed significant differences compared to the other three groups ($P < 0.001$, $P < 0.05$). However, the ZA-PRO group treated with PRO as a preventive measure showed significant improvement compared to the ZA group ($P < 0.05$, $P < 0.01$). Although there were no statistical differences in the Tb.N and Tb.Th among the groups throughout the process ($P > 0.05$), similar trends could still be observed (Fig. 3e).

Preventive effect of propranolol on BRONJ lesions as shown by histological analysis

For the histological examination of new bone formation, H&E and Masson trichrome stains were applied. Findings

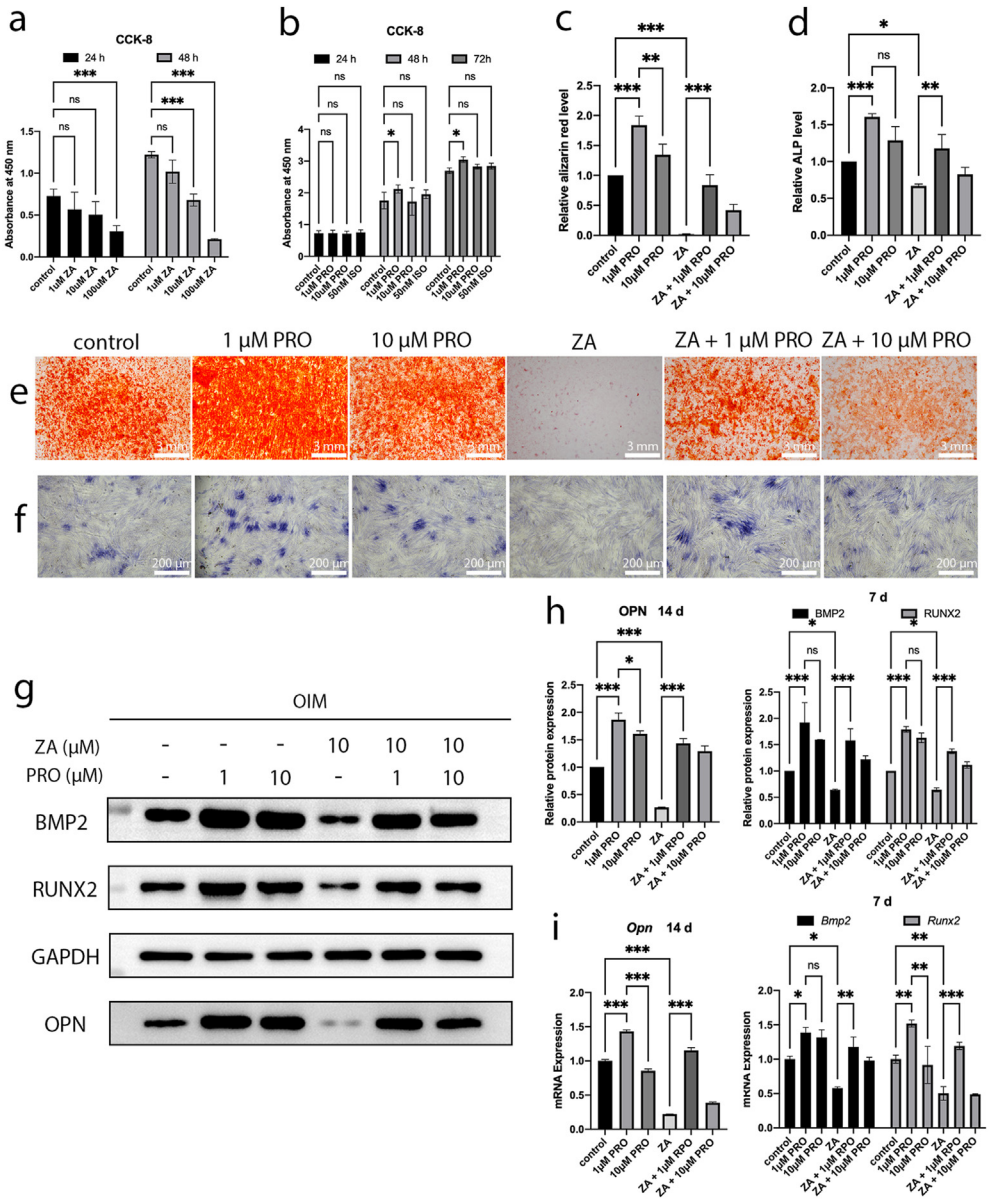

Figure 1 Effects of zoledronic acid (ZA) and propranolol (PRO) on cytotoxic and osteogenic differentiation on bone marrow mesenchymal stem cells (BMSCs). a) Quantitative cytotoxicity assay of ZA to BMSCs tested by CCK8 after 24 and 48 h. b) Quantitative cytotoxicity assay of PRO to BMSCs tested by CCK8 after 24, 48 and 72 h. c) Quantification of Alizarin red S staining. d) Quantification of alkaline phosphatase (ALP) staining. e) Alizarin red S staining of calcium deposits after treatments and osteoinduction for 21 days. Bar = 3 mm. f) ALP staining after treatments and osteoinduction for 14 days. Bar = 200 μm. g) Representative Western blot images of BMP2, RUNX2 (7 days), OPN (14 days) and GAPDH. OIM: osteogenic induction medium. h) Relative protein expression levels of BMP2, RUNX2 (7 days) and OPN (14 days) determined by Western blot. i) Relative mRNA expression levels of *Bmp2*, *Runx2* (7 days) and *Opn* (14 days) determined by RT-qPCR. Data are presented as means ± SD. $^{*}P < 0.05$, $^{**}P < 0.001$, $^{***}P < 0.001$.

revealed complete healing in both the control and PRO groups, characterized by mucosal healing and a rich quantity of cancellous bone that was interwoven to form a porous, reticular structure. Conversely, the ZA group exhibited poor repair and sparse trabeculae. Notably, an enhanced repair process was observed in the ZA-PRO group, where the extraction socket was substantially filled with new bone. Moreover, in the ZA-PRO group compared to the ZA group, the organization of both cancellous bone and collagen fibers appeared more developed, indicating a more mature bone structure (Fig. 4a–d). The other three groups showed much connective tissue and fibrous cells at the extraction site, while the ZA group showed local mucosal unhealing and strong inflammatory infiltration (Fig. 4b). In ZA group, the alveolar walls were characterized by necrotic bone tissue lacking osteocytes, surrounded by necrotic debris and bacteria. Conversely, in the control, PRO, and ZA-PRO groups, both the pre-existing bone tissues

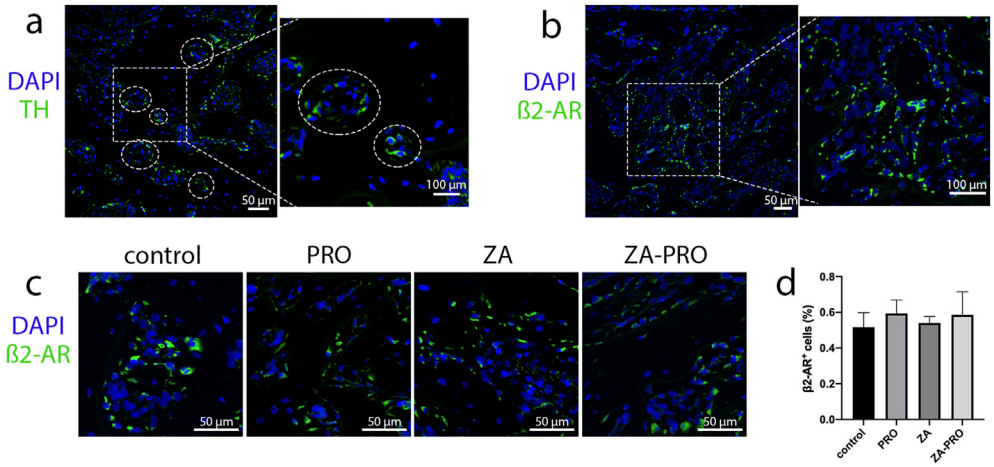

Figure 2 Sympathetic nervous system marker and β2-AR marker in the molar region. a) Tyrosine hydroxylase (TH)-positive (green) tissues in sections of tooth extraction socket, showing puncta structures around blood vessels (white circle). Bar = 50 μm. Bar = 100 μm. b) Localization of β2-AR (green) on cells of alveolar bone. Bar = 50 μm. Bar = 100 μm. c) Immunofluorescence staining of β2-AR (green) in alveolar bone across different groups. Bar = 50 μm. d) Quantitative analysis of the ratio of β2-AR-positive cells. Data are presented as means ± SD. $P > 0.05$.

within alveolar walls and neo-formed bone trabeculae can be observed (Fig. 4c).

This study assessed the percentage of empty osteocyte lacunae in the alveolar bone of different groups of mice, serving as an indicator of bone cellularity (Fig. 5a). The results demonstrated a significant increase in the percentage of empty osteocyte lacunae in the group treated with ZA compared to the other three groups ($P < 0.001$) (Fig. 5b). This finding suggests that ZA may contribute to a reduction in the number of osteocytes. Notably, mice treated with both ZA and PRO exhibited a significantly lower percentage of empty osteocyte lacunae compared to the ZA group ($P < 0.001$), indicating a potential reversal of ZA's effect by PRO.

Propranolol can upregulate the expression of osteogenic markers and reduced cell apoptosis after tooth extraction

In order to further understand the effect of PRO on mouse bone tissue, this study detected osteogenic related proteins through immunofluorescence staining. We found that the number of ALP^+ cells (Fig. 6a), $BMP2^+$ cells (Fig. 6b), and $RUNX2^+$ cells (Fig. 6c) in ZA group were significantly less than that in control and PRO groups ($P < 0.05$, $P < 0.05$, $P < 0.001$, respectively), whereas ZA-PRO group showed more expression of these osteogenic markers compared with the ZA group ($P < 0.001$).

During the healing period of the extraction socket, a certain amount of TUNEL staining was observed in the extraction socket. The groups treated with ZA (ZA group and ZA-PRO group) exhibited a higher number of $TUNEL^+$ cells, unlike control and PRO groups, which showed fewer $TUNEL^+$ cells (Fig. 6d). Despite the ZA-PRO group having higher TUNEL staining than both the control and PRO groups, the beneficial effect of PRO treatment was evident. Specifically, $TUNEL^+$ cells in the ZA-PRO group were less than that in the ZA group, and the difference was statistically significant ($P < 0.05$).

Discussion

The innervation of SNS to bone tissue and cells is the histological basis for its regulation of bone metabolism. Sympathetic nerve fibers are distributed in the periosteum, trabeculae, and bone marrow cavity, with the most abundant and densest distribution around the growth plate and the epiphysis of long bones.[27] Within the cortical bone, nerve fibers are arranged along the Haversian system and travel with blood vessels; in the cancellous bone and bone marrow cavity, most nerve fibers accompany blood vessels, with some distributed sporadically.[28] In this study, we have confirmed the presence of sympathetic nerves in the alveolar bone using immunofluorescence technology, laying the foundation for our research.

Currently, research into the prevention and treatment of MRONJ is ongoing.[29,30] Beyond surgical interventions, there are also related pharmacological treatments available, such as Teriparatide, which has been used in treating MRONJ. Teriparatide (FORTEO, Lilly, Cambridge, MA, USA), a recombinant form of parathyroid hormone, as the sole bone anabolic agent that the FDA has authorized for treating osteoporosis induced by glucocorticoids. It stimulates new bone formation on trabecular and cortical (periosteal and/or endosteal) bone surfaces by preferential stimulation of osteoblastic activity.[31] Therefore, Teriparatide treats MRONJ by promoting bone anabolic metabolism, based on the hypothesis of bone reconstruction disorder. However, its use in clinical practice is somewhat limited due to the risk of inducing osteosarcoma and its high cost.[32,33] Similarly, propranolol, as a beta-adrenergic receptor blocker, has shown good bone-forming effects. Hence, we aim to observe whether propranolol can stimulate bone anabolic metabolism, thereby preventing the occurrence of MRONJ.

Osteoblasts are crucial in bone development, restructuring, and the mending of bone lesions.[34] BPs directly impede osteoblast activity, which is a key factor in the onset of BRONJ.[35,36] It has been observed that both the

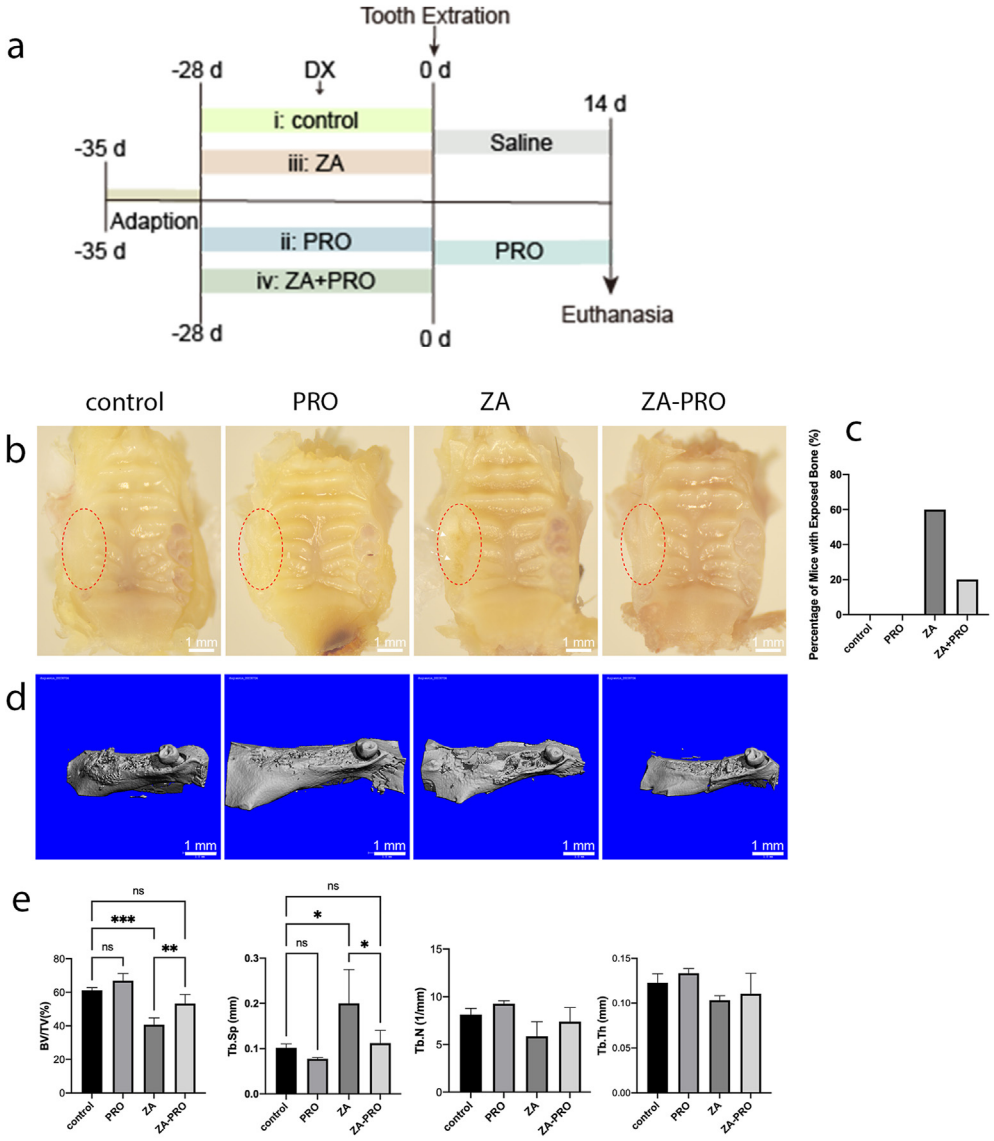

Figure 3 Propranolol prevented the occurrence of BRONJ. a) Schematic of the establishment of BRONJ animal model and drug injection process. DX: dexamethasone (2 mg/kg, i.p., twice a week). PRO: propranolol (20 mg/kg, i.p., twice a week). ZA: zoledronic acid (200 μg/kg, i.p., twice a week). b) Gross view of tooth extraction wound 2 weeks after operation. Bar = 1 mm. c) Mucosal healing rate. d) Representative micro-CT images. Bar = 1 mm. e) Statistical results of the ratio of bone volume to tissue volume (BV/TV), trabecular space (Tb.Sp), trabecular numbers (Tb.N) and trabecular thickness (Tb.Th) of tooth extraction sockets at 2 weeks. Data are presented as means ± SD. $^{*}P < 0.05$, $^{**}P < 0.01$, $^{***}P < 0.001$.

growth and the colony-forming efficiency of BMSCs in the vicinity of BRONJ lesions are markedly reduced compared to those in individuals without the condition.[11] Studies by Giannasi et al. have shown that BPs can inhibit the activity of osteoblast alkaline phosphatase and reduce the deposition of mineral nodules.[37] Manzano-Moreno et al. have demonstrated through in vitro experiments that high concentrations of BPs (≥10 mol/L) can alter the expression of essential genes in osteoblasts, block their cell cycle, and induce apoptosis and necrosis.[38] In our study, due to the administration of PRO, the ZA-PRO group showed an increase in the expression of factors related to osteogenic differentiation (RUNX2, BMP-2, and ALP). The recruitment and differentiation of osteoblasts stimulate the receptor activator of NF-κB ligand and colony-stimulating factor-1, promoting bone formation and altering the function of osteoclasts.[39–41] Therefore, by administering PRO, the balance between bone formation and resorption in the tooth extraction socket was restored, promoting its remodeling.

Although the pathogenesis of bone necrosis is not fully understood, evidence suggests that bisphosphonates may play a role by inhibiting endothelial cell proliferation and downregulating growth factors associated with angiogenesis, thereby reducing blood vessel formation. An in vivo study by Zhao et al. showed that rats injected i.p. with ZA experienced a reduction in the number of blood vessels in the alveolar sockets post molar extraction compared to the

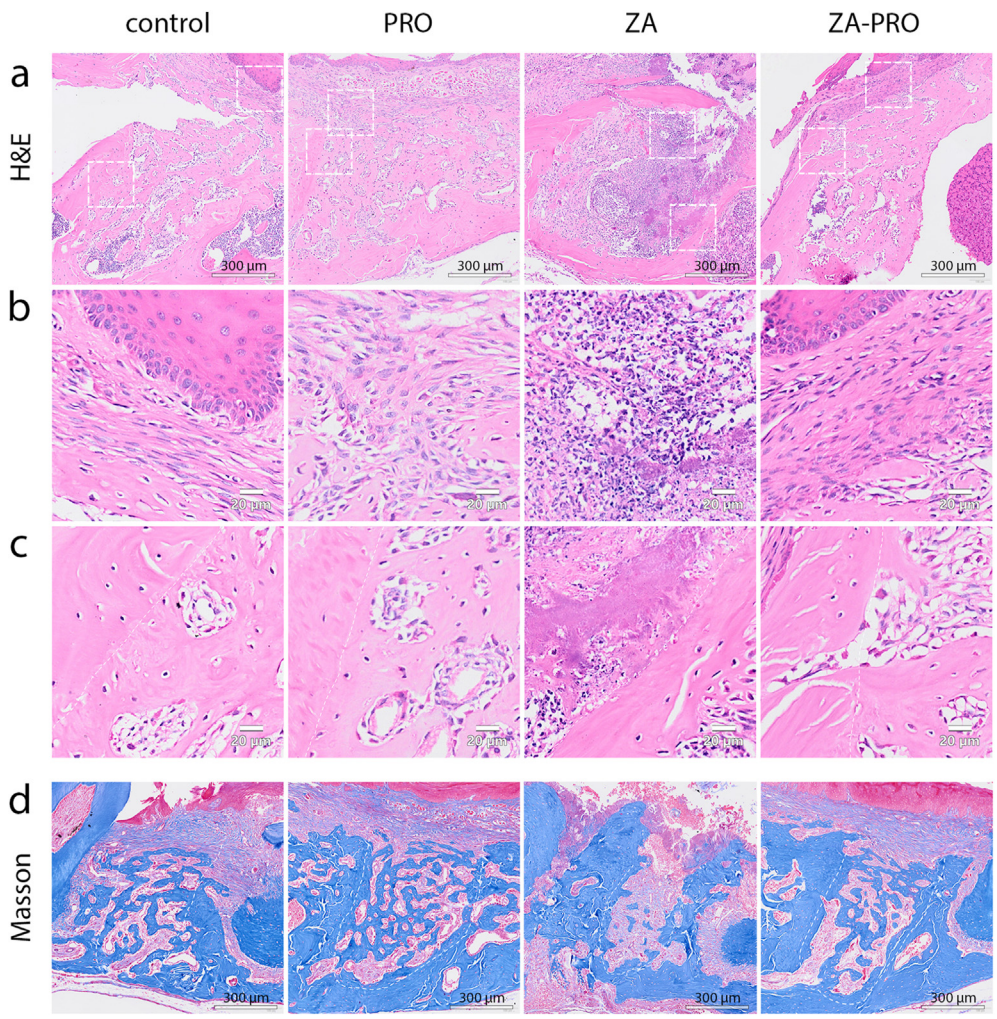

Figure 4 Histopathological results of hematoxylin and eosin (H&E) staining and Masson staining. a) Representative pictures of the mandibular tooth extraction sockets 2 weeks after operation (H&E. Bar = 300 μm). b) Representative pictures of the lamina propria of the mucosa overlying the tooth extraction sockets (H&E. Bar = 20 μm). c) Representative pictures of the alveolus wall and the neo-formed bone trabeculae in tooth extraction sockets (H&E. Bar = 20 μm). d) Representative pictures of the mandibular tooth extraction sockets 2 weeks after operation (Masson. Bar = 300 μm).

control group.[42] However, rats treated with pro-angiogenic materials demonstrated significant vascular improvement in the alveolar sockets compared to the ZA group. Propranolol, a beta-adrenergic receptor blocker known to inhibit angiogenesis.[43] Its effects on the alveolar bone and periodontal tissues are of interest to us. A separate experiment involved administering ISO and PBS to mice via intraperitoneal injection and subsequently examining vascular-related changes in the mandible and tibia. The findings indicated similar sympathetic innervation and adrenergic receptor, beta 2 mRNA expression in the jaw and tibial tissues. However, ISO treatment did not enhance either vascular area or number within any studied regions (dental pulp, periodontal ligament, and alveolar bone), nor did it alter vascular endothelial growth factor A expression in the mandibular molar region.[44] These findings indicate that the reaction of blood vessels to β-AR stimulants varies between tibial tissues and jawbone, showing that the angiogenic effect of SNS activity present in long bone is not evident in alveolar bone. This variance in response could be attributed to their different embryonic origins; craniofacial bones develop from neural crest cells through intramembranous ossification, whereas long bones are derived from mesodermal cells and undergo endochondral ossification.[45] Additionally, varying responses to catecholaminergic pathway stimulators or inhibitors have been observed across different periosteal regions, such as the femur and various parts of the mandible (alveolar wall, periosteum, post-molar endosteum), highlighting further differences in tissue response.[46] A specific dose of propranolol may exert an osteogenic effect in bone tissue, potentially by impacting the microenvironment between bone cells and vascular cells. Böhrnsen et al. found that in co-culture, BMSCs exhibited supportive expression for angiogenic function, while human umbilical vein endothelial cells enhanced the expression of osteogenic markers in BMSCs.[47] This suggests that propranolol may not exhibit vascular inhibitory effects in bone tissue because it promotes the proliferation and differentiation of BMSCs, thereby upregulating the expression of markers associated with

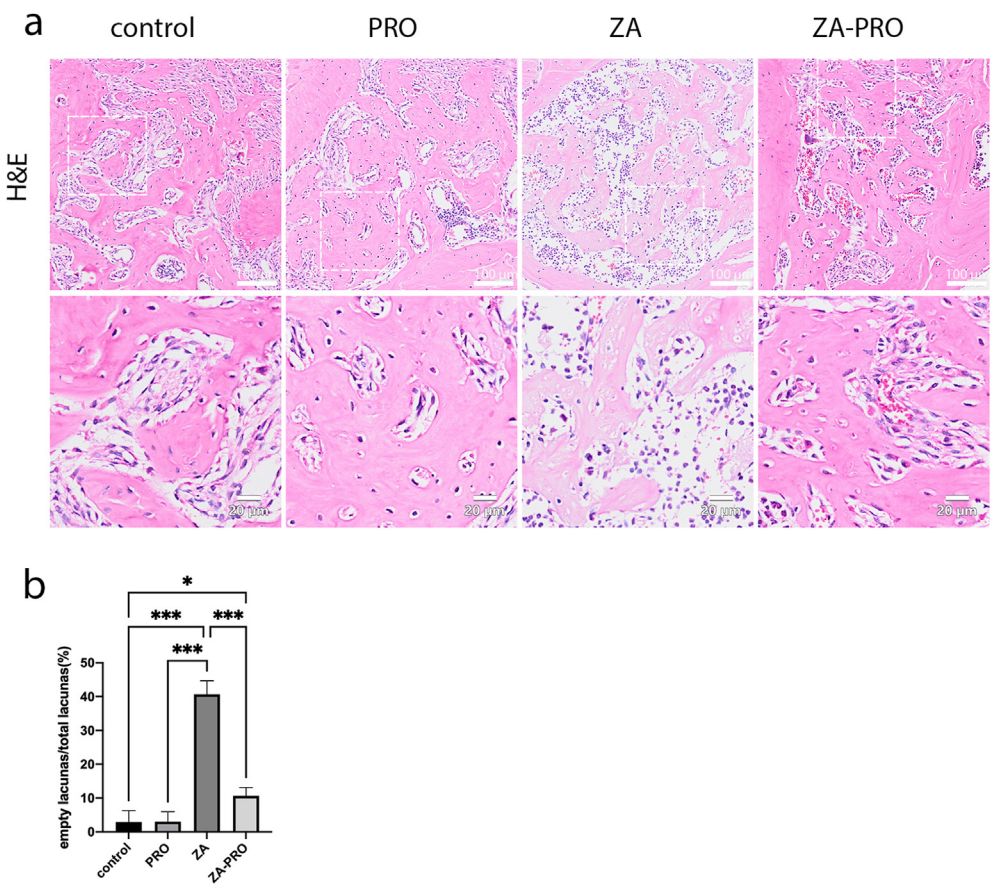

Figure 5 Zoledronic acid (ZA) induced more empty osteocyte lacunae in the alveolar bone. a) Representative pictures of osteocyte lacunae and empty osteocyte lacunae in tooth extraction sockets and alveolus wall (H&E. Bar = 100 μm. Bar = 20 μm). b) Statistical result of the percentage of empty osteocyte lacunae in different groups. Data are presented as means ± SD. *$P < 0.05$, ***$P < 0.001$.

angiogenesis. Unresolved are the questions regarding the timing and methodology through which the coordinated pattern of nerves and blood vessels is restored during the intricate and sequential processes of bone regeneration.[48] Further in vitro and in vivo experiments would be a potential direction for future research.

In histological evaluations using HE and Masson staining, we observed that the control and PRO groups presented similar outcomes, with the alveolar sockets nearly filled with newly formed bone. This observation is due to the fact that the detection time point was two weeks after the tooth extraction. In C57BL/6 mice, the extraction site of the maxillary first molar shows complete soft tissue healing and restoration of normal color and morphology with indistinct boundaries from surrounding tissues by day 14 post-extraction. At this time, the socket is fully filled with new bone; however, this new bone has a significantly lower density compared to the surrounding normal alveolar bone, with clear demarcation and containing numerous capillaries, but with disorganized trabecular patterns.[49] The results for the control and PRO groups in this study were consistent with these observations. Thus, at the 2-week post-extraction point, it may not be possible to discern a significant difference in the amount of new bone formation between the PRO and control groups. Nonetheless, the ZA group did not achieve ideal bone healing after 2 weeks, whereas the ZA-PRO group showed improvement. Furthermore, subsequent immunofluorescence staining analysis revealed higher expression of osteogenic markers within the PRO group's alveolar sockets compared to the control group, with statistical significance ($P < 0.01$). Typically, studies on alveolar socket healing employ more frequent observation intervals, such as days 1, 3, 7, 10, and 14 post-extraction.[50–53] In contrast, experiments designed to model BRONJ utilize longer sampling times due to the extended period required for necrotic bone formation, with intervals at 2 weeks,[54] 3 weeks,[55] 6 weeks,[56] and 8 weeks.[57,58] Considering this, we propose that the experimental design could be improved. Adhering to the "3Rs" principle (replacement, reduction, and refinement), additional time points could be reasonably included, such as regular in vivo micro-CT scans to assess bone healing, thereby yielding more comprehensive research data. However, conducting micro-CT scans in vivo may introduce variability due to the animals' respiratory movements. We hypothesize that the observed discrepancies between different experiments may be attributed to variables such as different animals, different sexual distinction, varying healing periods, and differing treatment durations. Consequently, there is a need to develop a standardized BRONJ

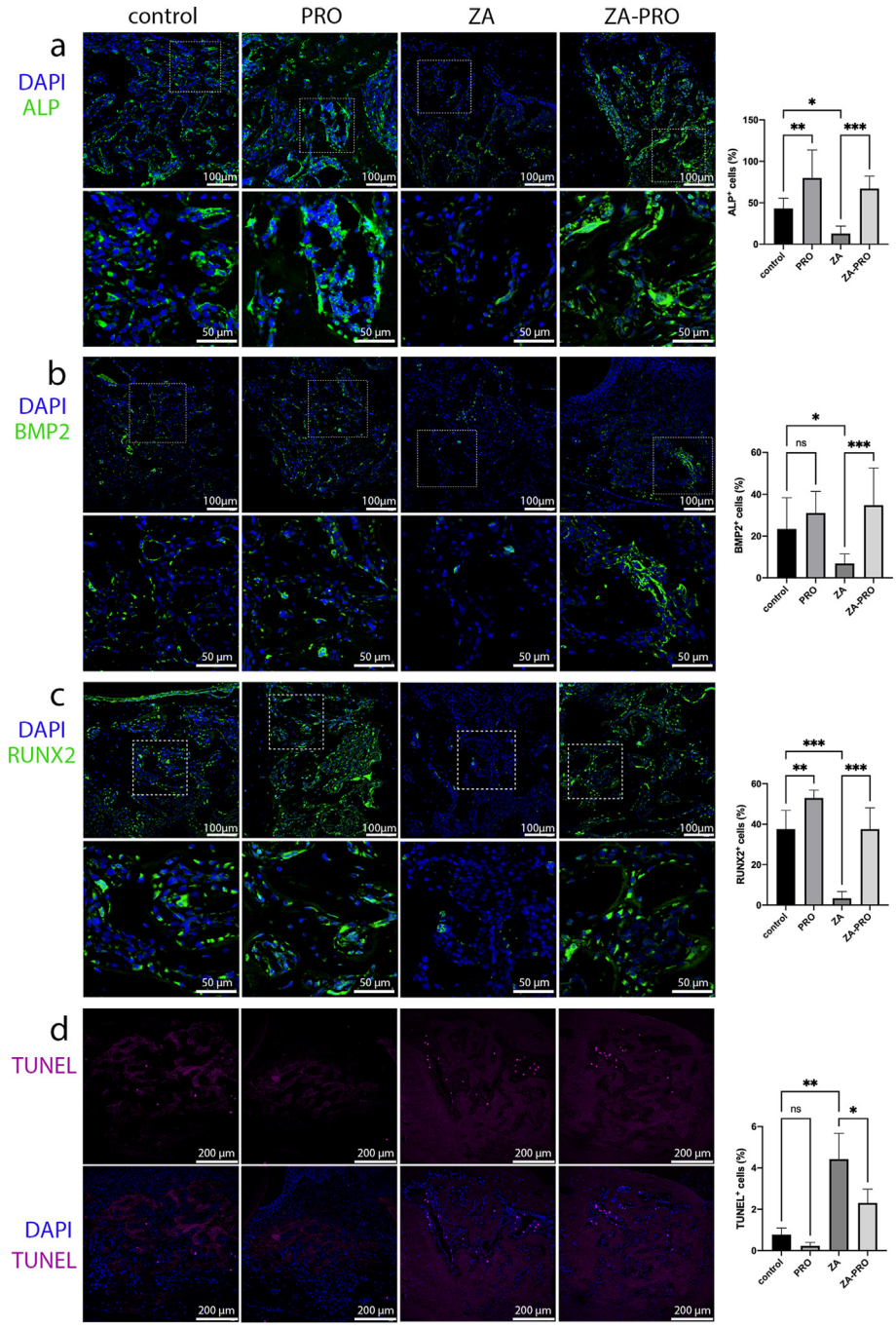

Figure 6 Propranolol promoted osteogenesis and reduced cell apoptosis in tooth extraction sockets. a-c) The immunofluorescence staining of ALP, BMP2, RUNX2 (green) in the tooth extraction sockets tissues at 2 weeks and quantitative analysis of ratio of positive cells. Bar = 100 μm. Bar = 50 μm. d) TUNEL staining (purple) in the tooth extraction sockets tissues at 2 weeks and quantitative analysis of ratio of TUNEL positive cells. Bar = 200 μm. Data are presented as means ± SD. *$P < 0.05$, **$P < 0.01$, ***$P < 0.001$.

animal model to facilitate consistent and reproducible results.

Propranolol is a well-established medication used in the management of cardiovascular conditions. Common adverse reactions can include bradycardia, hypotension, dizziness, and congestive heart failure. Clinical studies have explored the role of propranolol in the prevention and improvement of osteoporosis, specifically within the patient population suffering from cardiovascular diseases.[24,59] It is known that oral administration of 10 mg/kg of propranolol daily can lower blood pressure in obese mice.[60] In our animal research, mice administered 20 mg/kg of propranolol intraperitoneally exhibited transient symptoms such as rapid and deep breathing, limb weakness, and sluggish movement within an hour after injection, which are indicative of hypotension. Subsequently,

supportive care including fluid infusion and maintaining body temperature was provided to mitigate adverse effects in animals. Prior studies have also used a 20 mg/kg concentration of propranolol in rodent models to examine its effects on bone tissue,[61,62] while other research has utilized various concentrations and methods of administration.[63,64] Since this study is the first to apply propranolol in the BRONJ model, the drug's efficacy was previously unclear, thus we only used single concentration and method of administration for initial exploration. Given the adverse reactions observed in animals during the experiment, we believe that it is necessary to further explore suitable concentrations and methods of administration. When β-AR blockers are used for localized bone quality control, methods such as local injection and the use of slow-release materials may yield better outcomes. These methods can potentially reduce systemic reactions and increase local drug concentration. Research has shown that synthetic porous slow-release materials releasing propranolol locally can inhibit the detrimental effects of SNS activation on bone regeneration and effectively promote the healing of bone defects.[65,66]

In conclusion, propranolol has potential preventive and therapeutic effects on BRONJ by promoting bone formation. Pharmacological β-AR inhibition may be a new approach to treating BRONJ.

Declaration of competing interest

The authors have no conflicts of interest relevant to this article.

Acknowledgments

This study was supported by the Health Commission of Sichuan Province (ZH2024-901), Sichuan Science and Technology Program (2023ZYD0110), and Research and Develop Program, West China Hospital of Stomatology Sichuan University (RD-03-202405).

References

1. Russell RG. Bisphosphonates: the first 40 years. *Bone* 2011;49:2—19.
2. Advisory Task Force on Bisphosphonate-Related Osteonecrosis of the Jaws. American Association of Oral and Maxillofacial Surgeons position paper on bisphosphonate-related osteonecrosis of the jaws. *J Oral Maxillofac Surg* 2007;65:369—76.
3. Ruggiero SL, Dodson TB, Fantasia J, et al. American Association of Oral and Maxillofacial Surgeons position paper on medication-related osteonecrosis of the jaw-2014 update. *J Oral Maxillofac Surg* 2014;72:1938—56.
4. Coleman R, Woodward E, Brown J, et al. Safety of zoledronic acid and incidence of osteonecrosis of the jaw (ONJ) during adjuvant therapy in a randomised phase III trial (AZURE: BIG 01-04) for women with stage II/III breast cancer. *Breast Cancer Res Treat* 2011;127:429—38.
5. Lopez-Olivo MA, Shah NA, Pratt G, Risser JM, Symanski E, Suarez-Almazor ME. Bisphosphonates in the treatment of patients with lung cancer and metastatic bone disease: a systematic review and meta-analysis. *Support Care Cancer* 2012;20:2985—98.
6. Mauri D, Valachis A, Polyzos IP, Polyzos NP, Kamposioras K, Pesce LL. Osteonecrosis of the jaw and use of bisphosphonates in adjuvant breast cancer treatment: a meta-analysis. *Breast Cancer Res Treat* 2009;116:433—9.
7. Ng TL, Tu MM, Ibrahim MFK, et al. Long-term impact of bone-modifying agents for the treatment of bone metastases: a systematic review. *Support Care Cancer* 2021;29:925—43.
8. He Y, Chen H, An JG, et al. Expert consensus on diagnosis and clinical management of medication-related osteonecrosis of the jaw. *China J Oral Maxillofac Surg* 2023;21:313—25 [In Chinese, English abstract].
9. Pan J, Liu JY. Mechanism, prevention, and treatment for medication-related osteonecrosis of the jaws. *West China J Stomatol* 2021;39:245—54 [In Chinese, English abstract].
10. Rogers MJ, Gordon S, Benford HL, et al. Cellular and molecular mechanisms of action of bisphosphonates. *Cancer* 2000;88:2961—78.
11. He LH, Xiao E, An JG, et al. Role of bone marrow stromal cells in impaired bone repair from BRONJ osseous lesions. *J Dent Res* 2017;96:539—46.
12. Su ZF, Li JH, Bai X, et al. Borate bioactive glass prevents zoledronate-induced osteonecrosis of the jaw by restoring osteogenesis and angiogenesis. *Oral Dis* 2020;26:1706—17.
13. Cui YJ, Zhang WD, Yang PP, Zhu SQ, Luo SL, Li MQ. Menaquinone-4 prevents medication-related osteonecrosis of the jaw through the SIRT1 signaling-mediated inhibition of cellular metabolic stresses-induced osteoblast apoptosis. *Free Radical Biol Med* 2023;206:33—49.
14. Ning HR, Wu XW, Wu Q, et al. Microfiber-reinforced composite hydrogels loaded with rat adipose-derived stem cells and BMP-2 for the treatment of medication-related osteonecrosis of the jaw in a rat model. *ACS Biomater Sci Eng* 2019;5:2430—43.
15. Takeda S, Elefteriou F, Levasseur R, et al. Leptin regulates bone formation via the sympathetic nervous system. *Cell* 2002;111:305—17.
16. Fu LN, Patel MS, Bradley A, Wagner EF, Karsenty G. The molecular clock mediates leptin-regulated bone formation. *Cell* 2005;122:803—15.
17. Elefteriou F, Ahn JD, Takeda S, et al. Leptin regulation of bone resorption by the sympathetic nervous system and CART. *Nature* 2005;434:514—20.
18. Martín-Escudero JC, Pérez-Castrillón JL, Blanco FS, Arzua-Mouronte D, Bellido Casado J, Martín JM. Relation between bone mass and catecholamines in the general population. *Horm Res* 2007;68:63—7.
19. Hajifathali A, Saba F, Atashi A, Soleimani M, Mortaz E, Rasekhi M. The role of catecholamines in mesenchymal stem cell fate. *Cell Tissue Res* 2014;358:651—65.
20. Li JY, Zhang ZY, Tang JR, Hou ZY, Li LJ, Li B. Emerging roles of nerve-bone axis in modulating skeletal system. *Med Res Rev* 2024:1—37.
21. Pierroz DD, Bonnet N, Bianchi EN, et al. Deletion of beta-adrenergic receptor 1, 2, or both leads to different bone phenotypes and response to mechanical stimulation. *J Bone Miner Res* 2012;27:1252—62.
22. Cao H, Kou X, Yang R, et al. Force-induced Adrb2 in periodontal ligament cells promotes tooth movement. *J Dent Res* 2014;93:1163—9.
23. Sun JL, Yan JF, Li J, et al. Conditional deletion of Adrb2 in mesenchymal stem cells attenuates osteoarthritis-like defects in temporomandibular joint. *Bone* 2020;133:115229.
24. Schlienger RG, Kraenzlin ME, Jick SS, Meier CR. Use of β-blockers and risk of fractures. *JAMA* 2004;292:1326—32.
25. Al-Subaie AE, Laurenti M, Abdallah MN, et al. Propranolol enhances bone healing and implant osseointegration in rats tibiae. *J Clin Periodontol* 2016;43:1160—70.
26. Yan R, Jiang RX, Hu LW, Deng YW, Wen J, Jiang XQ. Establishment and assessment of rodent models of medication-

related osteonecrosis of the jaw (MRONJ). *Int J Oral Sci* 2022; 14:41.
27. Serre CM, Farlay D, Delmas PD, Chenu C. Evidence for a dense and intimate innervation of the bone tissue, including glutamate-containing fibers. *Bone* 1999;25:623—9.
28. Duncan CP, Shim SSJ. Edouard Samson address: the autonomic nerve supply of bone. An experimental study of the intraosseous adrenergic nervi vasorum in the rabbit. *J Bone Joint Surg Br* 1977;59:323—30.
29. Chopra K, Malhan N. Teriparatide for the treatment of medication-related osteonecrosis of the jaw. *Am J Therapeut* 2020;28:e469—77.
30. Sim IW, Borromeo GL, Tsao C, et al. Teriparatide promotes bone healing in medication-related osteonecrosis of the jaw: a placebo-controlled, randomized trial. *J Clin Oncol* 2020;38: 2971—80.
31. Eli Lilly and Company. *FORTEO- teriparatide injection, solution*. Cambridge, MA: Eli Lilly and Company; 2021. Available at: https://uspl.lilly.com/forteo/forteo.html#pi. [Accessed 4 February 2024] [Date accessed.
32. Watanabe A, Yoneyama S, Nakajima M, et al. Osteosarcoma in Sprague-Dawley rats after long-term treatment with teriparatide (human parathyroid hormone (1-34)). *J Toxicol Sci* 2012; 37:617—29.
33. Subbiah V, Madsen VS, Raymond AK, Benjamin RS, Ludwig JA. Of mice and men: divergent risks of teriparatide-induced osteosarcoma. *Osteoporos Int* 2010;21:1041—5.
34. Xiao CW, Zhou HF, Liu GP, et al. Bone marrow stromal cells with a combined expression of BMP-2 and VEGF-165 enhanced bone regeneration. *Biomed Mater* 2011;6:015013.
35. Kellinsalmi M, Mönkkönen H, Mönkkönen J, et al. In vitro comparison of clodronate, pamidronate and zoledronic acid effects on rat osteoclasts and human stem cell-derived osteoblasts. *Basic Clin Pharmacol Toxicol* 2010;97:382—91.
36. Borsani E, Bonazza V, Buffoli B, et al. Beneficial effects of concentrated growth factors and resveratrol on human osteoblasts in vitro treated with bisphosphonates. *BioMed Res Int* 2018;2018:4597321.
37. Giannasi C, Niada S, Farronato D, et al. Nitrogen containing bisphosphonates impair the release of bone homeostasis mediators and matrix production by human primary pre-osteoblasts. *Int J Med Sci* 2019;16:23—32.
38. Manzano-Moreno FJ, Ramos-Torrecillas J, Melguizo-Rodríguez L, Illescas-Montes R, Ruiz C, García-Martínez O. Bisphosphonate modulation of the gene expression of different markers involved in osteoblast physiology: possible implications in bisphosphonate-related osteonecrosis of the jaw. *Int J Med Sci* 2018;15:359—67.
39. Dougall WC, Glaccum M, Charrier K, et al. RANK is essential for osteoclast and lymph node development. *Genes Dev* 1999;13: 2412—24.
40. Kong YY, Feige U, Sarosi I, et al. Activated T cells regulate bone loss and joint destruction in adjuvant arthritis through osteoprotegerin ligand. *Nature* 1999;402:304—9.
41. Van Wesenbeeck L, Odgren PR, MacKay CA, et al. The osteopetrotic mutation toothless (tl) is a loss-of-function frameshift mutation in the rat Csf1 gene: evidence of a crucial role for CSF-1 in osteoclastogenesis and endochondral ossification. *Proc Natl Acad Sci U S A* 2002;99:14303—8.
42. Zhao D, Xiao DX, Liu MT, et al. Tetrahedral framework nucleic acid carrying angiogenic peptide prevents bisphosphonate-related osteonecrosis of the jaw by promoting angiogenesis. *Int J Oral Sci* 2022;14:23.
43. Wu HW, Wang X, Liang H, Zheng JW, Huang SY, Zhang DS. Enhanced efficacy of propranolol therapy for infantile hemangiomas based on a mesoporous silica nanoplatform through mediating autophagy dysfunction. *Acta Biomater* 2020;107:272—85.
44. Moraes RM, Elefteriou F, Anbinder AL. Response of the periodontal tissues to β-adrenergic stimulation. *Life Sci* 2021;281: 119776.
45. Couly GF, Coltey PM, Le Douarin NM. The triple origin of skull in higher vertebrates: a study in quail-chick chimeras. *Development* 1993;117:409—29.
46. Bataille C, Mauprivez C, Haÿ E, et al. Different sympathetic pathways control the metabolism of distinct bone envelopes. *Bone* 2012;50:1162—72.
47. Böhrnsen F, Schliephake H. Supportive angiogenic and osteogenic differentiation of mesenchymal stromal cells and endothelial cells in monolayer and co-cultures. *Int J Oral Sci* 2016;8: 223—30.
48. Tao RY, Mi BB, Hu YQ, et al. Hallmarks of peripheral nerve function in bone regeneration. *Bone Res* 2023;11:6.
49. Liang BL, Zhang WY, Xue Y, et al. Observation and analysis of tooth extraction wound healing process of maxillary first molars in C57B/6 mice. *Chin J Pract Stomatol* 2019;12:232—6 [In Chinese, English abstract].
50. Cao ZW, Shi HT, Hu LR, Zhang K, Zhang XH, Pan J. Yes-associated protein promotes bone healing after tooth extraction in mice. *Biochem Biophys Res Commun* 2022;609:39—47.
51. Jiang F, Yang XH, Meng X, Zhou ZX, Chen N. Effect of CBX7 deficiency on the socket healing after tooth extractions. *J Bone Miner Metabol* 2019;37:584—93.
52. Fujii S, Takebe H, Mizoguchi T, Nakamura H, Shimo T, Hosoya A. Bone formation ability of $Gli1^{+}$ cells in the periodontal ligament after tooth extraction. *Bone* 2023;173: 116786.
53. Min KK, Neupane S, Adhikari N, et al. Effects of resveratrol on bone-healing capacity in the mouse tooth extraction socket. *J Periodontal Res* 2020;55:247—57.
54. Okawa H, Kondo T, Hokugo A, et al. Fluorescent risedronate analogue 800CW-pRIS improves tooth extraction-associated abnormal wound healing in zoledronate-treated mice. *Commun Med* 2022;2:112.
55. Song MJ, Alshaikh A, Kim T, et al. Preexisting periapical inflammatory condition exacerbates tooth extraction—induced bisphosphonate-related osteonecrosis of the jaw lesions in mice. *J Endod* 2016;42:1641—6.
56. Soma T, Iwasaki R, Sato Y, et al. Osteonecrosis development by tooth extraction in zoledronate treated mice is inhibited by active vitamin D analogues, anti-inflammatory agents or antibiotics. *Sci Rep* 2022;12:19.
57. Soundia A, Hadaya D, Esfandi N, et al. Osteonecrosis of the jaws (ONJ) in mice after extraction of teeth with periradicular disease. *Bone* 2016;90:133—41.
58. Vitale M, Corrêa MG, Ervolino E, et al. Resveratrol for preventing medication-related osteonecrosis of the jaws in rats. *Oral Dis* 2023;00:1—13.
59. Graham S, Hammond-Jones D, Gamie Z, Polyzois I, Tsiridis E, Tsiridis E. The effect of β-blockers on bone metabolism as potential drugs under investigation for osteoporosis and fracture healing. *Expet Opin Invest Drugs* 2008;17: 1281—99.
60. da Silva Franco N, Lubaczeuski C, Guizoni DM, et al. Propranolol treatment lowers blood pressure, reduces vascular inflammatory markers and improves endothelial function in obese mice. *Pharmacol Res* 2017;122:35—45.
61. Hu CH, Sui BD, Liu J, et al. Sympathetic neurostress drives osteoblastic exosomal miR-21 transfer to disrupt bone homeostasis and promote osteopenia. *Small Methods* 2022;6: e2100763.
62. Jiao K, Niu LN, Li QH, et al. β2-Adrenergic signal transduction plays a detrimental role in subchondral bone loss of temporomandibular joint in osteoarthritis. *Sci Rep* 2015;5: 12593.

63. Huang J, Wu T, Jiang YR, et al. β-Receptor blocker enhances the anabolic effect of PTH after osteoporotic fracture. *Bone Res* 2024;12:18.
64. Folwarczna J, Pytlik M, Sliwiński L, Cegieła U, Nowińska B, Rajda M. Effects of propranolol on the development of glucocorticoid-induced osteoporosis in male rats. *Pharmacol Rep* 2011;63:1040—9.
65. Guo ST, He CL. Bioprinted scaffold remodels the neuromodulatory microenvironment for enhancing bone regeneration. *Adv Funct Mater* 2023;33:2304172.
66. Wu H, Song Y, Li JQ, et al. Blockade of adrenergic β-receptor activation through local delivery of propranolol from a 3D collagen/polyvinyl alcohol/hydroxyapatite scaffold promotes bone repair in vivo. *Cell Prolif* 2020;53:e12725.